Journal of Power and Energy Engineering, 2026, 14(9), 56-69
https://www.scirp.org/journal/jpee
ISSN Online: 2327-5901
ISSN Print: 2327-588X

Effect of Heat Treatment on Crystallite Size, Band-Gap Energy, and Photocatalytic Degradation of Brookite TiO_2 Thin Films

Jariah Mohamad Juoi[1], Nur Dalilah Johari[1], Zulkifli Mohd Rosli[2]

[1]Faculty of Industrial and Manufacturing Technology and Engineering, Universiti Teknikal Malaysia Melaka, Durian Tunggal, Melaka, Malaysia
[2]Sekolah Asasi Teknikal dan Pengajian Diploma, Universiti Teknikal Malaysia Melaka, Durian Tunggal, Melaka, Malaysia
Email: jariah@utem.edu.my

How to cite this paper: Juoi, J.M., Johari, N.D. and Rosli, Z.M. (2026) Effect of Heat Treatment on Crystallite Size, Band-Gap Energy, and Photocatalytic Degradation of Brookite TiO_2 Thin Films. *Journal of Power and Energy Engineering*, **14**, 56-69.
https://doi.org/10.4236/jpee.2026.149004

Received: August 21, 2026
Accepted: September 20, 2026
Published: September 23, 2026

Abstract

Brookite TiO_2 is less extensively investigated in thin-film photocatalysis than anatase and rutile, and its response to thermal processing remains of interest. Here, brookite TiO_2 coatings were produced by sol-gel spin coating and heat-treated at 200˚C, 300˚C, 400˚C, and 500˚C for 3 h. Glancing-angle X-ray diffraction (GAXRD), transmission electron microscopy with selected-area electron diffraction (TEM/SAED), UV-Vis spectroscopy, and methylene-blue (MB) degradation measurements were used to relate thermal history to structure, optical response, and photocatalytic behaviour. Brookite was the only detectable crystalline TiO_2 phase at 200˚C - 400˚C, whereas the 500˚C film showed a predominantly amorphous XRD pattern. The calculated crystallite size changed from 47.9 nm ± 19.9 nm at 200˚C to 58.4 nm ± 12.0 nm at 300˚C and then to 7.8 nm ± 1.0 nm at 400˚C. The estimated optical band gap varied from 3.37 to 3.90 eV, reaching its minimum at 300˚C. This sample also gave the highest four-hour MB removal, 67.7% under UV-C irradiation and 97.8% under the reported visible-light condition. The results indicate that the photocatalytic response follows the combined evolution of crystallinity, crystallite size, and optical band gap with annealing temperature. Within the investigated processing window, 300˚C provided the most favourable overall combination of measured properties and MB degradation performance.

Keywords

TiO_2, Crystallite Size, Band-Gap Energy, Thin Film, Methylene Blue, Photocatalytic Degradation

1. Introduction

TiO_2 is widely used as a photocatalyst because it offers a combination of chemical robustness, thermal stability, low material cost, broad availability, and comparatively low toxicity [1] [2]. The seminal photoelectrochemical water-splitting study by Fujishima and Honda [3] helped establish the foundation for subsequent TiO_2 photocatalysis. Three naturally occurring polymorphs are recognised that are anatase, rutile, and brookite. Their different crystal structures give rise to different electronic and surface characteristics. Anatase is often associated with strong photocatalytic activity, whereas rutile is the thermodynamically stable polymorph. Brookite is metastable and has received less attention, although its photocatalytic properties can differ appreciably from those of anatase and rutile [4] [5].

Research on TiO_2 has historically concentrated on anatase and rutile, partly because reproducible synthesis and phase control for these polymorphs are comparatively straightforward. In contrast, obtaining brookite as the principal phase is more challenging, and brookite commonly appears only as a minor constituent in conventional TiO_2 preparations [6]-[9]. Djaoued *et al.* [10], for example, reported less than 5% brookite in low-temperature dip-coated anatase films, whereas other synthesis strategies have produced brookite-rich material within more restricted processing ranges [11]. Reliable preparation of brookite-dominant coatings is consequently important for separating the influence of thermal treatment from that of phase composition. Despite its less established synthesis, brookite has demonstrated considerable photocatalytic promise. Kandiel *et al.* [12] found that brookite nanoparticles could outperform anatase and reported approximately twice the photonic efficiency, with brookite crystallites near 25 nm compared with approximately 4 nm for anatase. Tran *et al.* [13] likewise observed stronger degradation of ibuprofen, phenol, and cinnamic acid with brookite than with the corresponding anatase catalyst. Useful activity has also been reported for pure brookite thin films [14]. These results support treating brookite as a potentially effective photocatalyst rather than merely a secondary phase in anatase/rutile systems.

Photocatalytic performance cannot, however, be assigned to phase identity alone. Heat treatment can simultaneously alter crystallite dimensions, crystallinity, surface characteristics, defect populations, and the optical absorption edge. Changes in any of these parameters may influence adsorption, photocarrier generation or transport, and the availability of reactive surface sites. Consequently, comparing films across annealing temperatures requires the structural and optical measurements to be considered alongside the degradation results. Moreover, the literature contains substantially more work on brookite powders and mixed-phase materials than on brookite-dominant thin films prepared under a controlled thermal sequence. This work addresses that gap by examining spin-coated TiO_2 films for which brookite is the only crystalline TiO_2 phase detected at the lower heat-treatment temperatures. The films were treated at 200˚C, 300˚C, 400˚C, and 500˚C for 3 h. GAXRD and TEM/SAED were used to assess phase and microstructure, while UV-Vis measurements provided optical band-gap estimates. MB degradation was

then measured under UV-C and the reported visible-light condition. The purpose was to establish how thermal treatment changes the measured structural and optical descriptors and whether those changes are reflected in photocatalytic performance.

2. Materials and Methods

2.1. Preparation of TiO_2 Sol and Thin-Film Deposition

The precursor was titanium(IV) isopropoxide (TTIP, 97%, Sigma-Aldrich). A 0.2 M TTIP solution was made by adding TTIP to 64 mL of deionised water while stirring at room temperature. Hydrochloric acid (HCl, 37%; 0.4 mL) was subsequently introduced dropwise under continued stirring. After an additional 3 h of stirring, the sol was aged at room temperature for 48 h before use.

Glass substrates measuring 25.4 mm × 10.0 mm × 1.0 mm were cleaned successively with acetone, ethanol, and distilled water in an ultrasonic bath for 10 min. The substrates were then dried at 110˚C for 2 h. For coating, about 90 μL of aged sol was placed on each substrate and spin-coated under vacuum at 1500 rpm for 30 s, using a ramp rate of 500 rpm·s^{-1}. Each substrate received two coating cycles, followed by drying at 110˚C for 1 h.

The coated substrates were subsequently annealed for 3 h at four temperatures: 200˚C, 300˚C, 400˚C, and 500˚C. This temperature series was selected to track the effect of progressively stronger thermal treatment on phase constitution, microstructure, optical response, and MB-removal performance.

2.2. Characterisation of Brookite TiO_2 Thin Films

GAXRD measurements were obtained with a PANalytical X'Pert PRO MPD (PW 3060/60) instrument using Cu Kα radiation (λ = 1.5406 Å). The scans covered 2θ = 10˚ - 80˚ with a 4˚ incidence angle; the operating conditions were 40 kV and 30 mA. Phase identification was performed using X'Pert HighScore. The crystallite size was calculated from the principal brookite diffraction peak using the Scherrer equation:

$$D = \frac{k\lambda}{\beta \cos\theta} \tag{1}$$

Here, D is the mean coherent-domain dimension, k is the shape factor (0.94), λ is the Cu Kα wavelength (0.15406 nm), β is the FWHM expressed in radians, and θ is the Bragg angle. The principal diagnostic reflections for anatase, rutile, and brookite occur near 25˚, 27˚, and 31˚, respectively. Because only brookite reflections were detected from the 200˚C - 400˚C films, the brookite (111) peak near 31˚ was used for the size determination.

TEM examination was carried out with an HT-7700 transmission electron microscope at 120 kV. Micrographs were collected at magnifications of 600,000× to examine the film microstructure.

Optical absorption was measured from 200 to 1100 nm using a PerkinElmer Lambda 35 UV-Vis spectrophotometer. The optical band gap was estimated from

the Tauc representation, using the linear region of $(\alpha h\nu)^2$ versus $h\nu$ and extrapolating that region to the energy intercept. The resulting values should therefore be regarded as optical-edge estimates obtained from the measured spectra.

2.3. Photocatalytic Test

For photocatalytic evaluation, a 150 W germicidal UV-C lamp was positioned 16 cm from the solution. A coated film was placed in 35 mL of 1×10^{-6} M MB solution for each experiment. Before illumination, the suspension was kept in darkness for 30 min so that adsorption and desorption could approach equilibrium. Irradiation was then performed for 4 h, and samples were taken at 60 min intervals using separate beakers for absorbance measurements. The visible-light experiment reported in this work used a 200 W OSRAM model.

MB concentration was followed from the absorbance measured at 665 nm with a SHIMADZU UV-1700 UV-Vis spectrometer. Under the Beer-Lambert proportionality assumption, the percentage removal was calculated from either concentration or absorbance according to:

$$\text{MB degradation}(\%) = (C_0 - C)/C_0 \times 100 = (A_0 - A)/A_0 \times 100 \quad (2)$$

C_0 is the MB concentration after the dark-equilibration period, and C is the concentration at the selected irradiation time. A_0 and A denote the corresponding absorbances before and after irradiation, respectively.

3. Results

3.1. Characterization of TiO_2 Thin Films

The diffraction response changed markedly with heat-treatment temperature (**Figure 1**). At 200˚C, reflections assigned to brookite (111) and (023) occurred at approximately 31˚ and 66˚. The ~31˚ reflection gives a d-spacing of about 2.8 Å and is more consistent with JCPDS 84-1750 (31.3˚, 2.81 Å) than with JCPDS 29-1360 (30.8˚, 2.9 Å). After treatment at 300˚C and 400˚C, the brookite (111) reflection remained the only detectable crystalline TiO_2 peak and became weaker with increasing temperature. No distinct crystalline TiO_2 peak was resolved after treatment at 500˚C, so that specimen was classified as predominantly amorphous on the basis of XRD.

The progressive weakening of the brookite reflection is compatible with the metastability of brookite and its sensitivity to the chemical and thermal history of the precursor-derived coating. Earlier work indicates that brookite formation depends on nucleation conditions, crystallite dimensions, and possible deviations from ideal stoichiometry at both surfaces and within the material [15] [16]. Allen *et al.* [17] reported a comparable reduction in brookite fraction, from 39.7% at 110˚C to 15.1% at 600˚C, followed by loss of detectable brookite at still higher temperatures [18]. The present data therefore suggest that the selected thermal schedule can progressively reduce the stability or detectability of brookite in this particular film system.

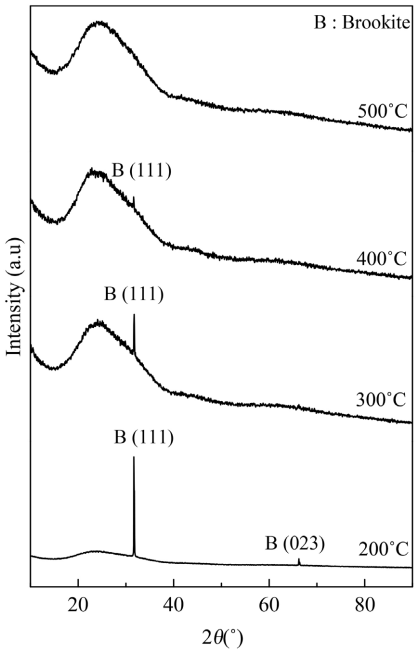

Figure 1. GAXRD patterns of spin-coated TiO_2 films after heat treatment at the indicated temperatures.

The amorphous appearance at 500˚C may also reflect the chemistry established during sol preparation. In the present procedure, TTIP was introduced at approximately one drop per minute, and HCl was used to influence hydrolysis and nucleation [19]. Solvent composition can modify precursor interactions and the hydrolysis/condensation sequence; differences between water- and methanol-containing systems have been reported [20]. Accordingly, the 500˚C observation should be linked to the complete processing route used here, rather than interpreted as a general rule for every TTIP-derived brookite coating.

Using the brookite (111) peak, the Scherrer analysis produced 47.9 nm ± 19.9 nm at 200˚C, 58.4 nm ± 12.0 nm at 300˚C, and 7.8 nm ± 1.0 nm at 400˚C (**Figure 2**). A size value was not assigned to the 500˚C specimen because its XRD pattern did not contain a sufficiently resolved brookite reflection.

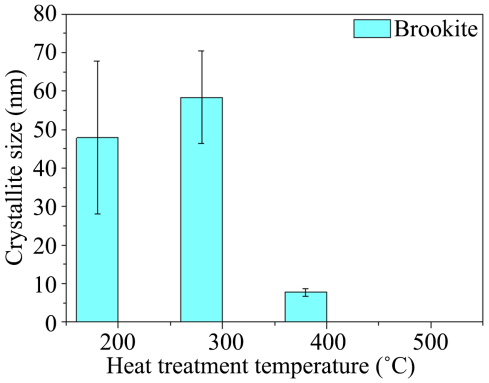

Figure 2. Crystallite size estimated from the brookite (111) reflection versus heat-treatment temperature.

The size increase between 200˚C and 300˚C suggests development of larger coherent diffracting regions during the initial stage of thermal treatment. This behaviour changed at 400˚C: the calculated value fell to 7.8 nm ± 1.0 nm while the brookite (111) intensity was strongly reduced. Such a reversal can be associated with destabilisation of brookite and a reduction in the size of coherently diffracting regions [21]. The measured sequence should therefore be described as non-monotonic rather than as continuous thermal grain growth.

Table 1 compiles the crystalline-phase assignments from GAXRD. Brookite was detected at 200˚C, 300˚C, and 400˚C, with no resolvable anatase or rutile reflections. At 500˚C, the pattern was predominantly amorphous and did not provide a reliable crystalline-phase assignment. Within this experimental window, the principal change at the highest treatment temperature was thus the disappearance of detectable brookite crystallinity rather than a demonstrable conversion to anatase or rutile.

Table 1. Detectable TiO_2 crystalline phases in the spin-coated films after heat treatment.

	Brookite (%)
200˚C	100.0
300˚C	100.0
400˚C	100.0
500˚C	Not determined; predominantly amorphous

3.2. Transmission Electron Microscopy

TEM and SAED results for the 200˚C and 300˚C films are presented in Figure 3. At 200˚C, the film contained mainly near-spherical features and lattice fringes of approximately 0.28 nm, matching the brookite (111) assignment obtained from GAXRD. The corresponding SAED pattern was also compatible with brookite. After treatment at 300˚C, the observed morphology was more sheet-like; nevertheless, the ~0.28 nm spacing persisted, and the SAED pattern continued to support the brookite assignment.

3.3. UV-Vis Optical Properties and Band-Gap Energy

Figure 4 shows the UV-Vis response of the films between 250 and 700 nm. A strong absorption feature centred near 280 nm was present for all specimens, in agreement with previously reported brookite TiO_2 behaviour [22] [23]. Tauc plots were used to estimate the optical band gap from the linear portion of the $(\alpha h\nu)^2$ versus $h\nu$ relationship. The resulting intercepts were compared to determine how the optical edge varied with thermal treatment.

The calculated optical gaps were 3.42 eV (200˚C), 3.37 eV (300˚C), 3.55 eV (400˚C), and 3.90 eV (500˚C). Thus, the band gap reached a minimum at 300˚C and subsequently widened. The 200˚C - 400˚C values fall within the range reported for brookite TiO_2 [5]. The changes may reflect temperature-dependent microstructural disorder and defect-related electronic states, which have previously been associated with shifts in TiO_2 optical-gap behaviour [24] (Figure 5).

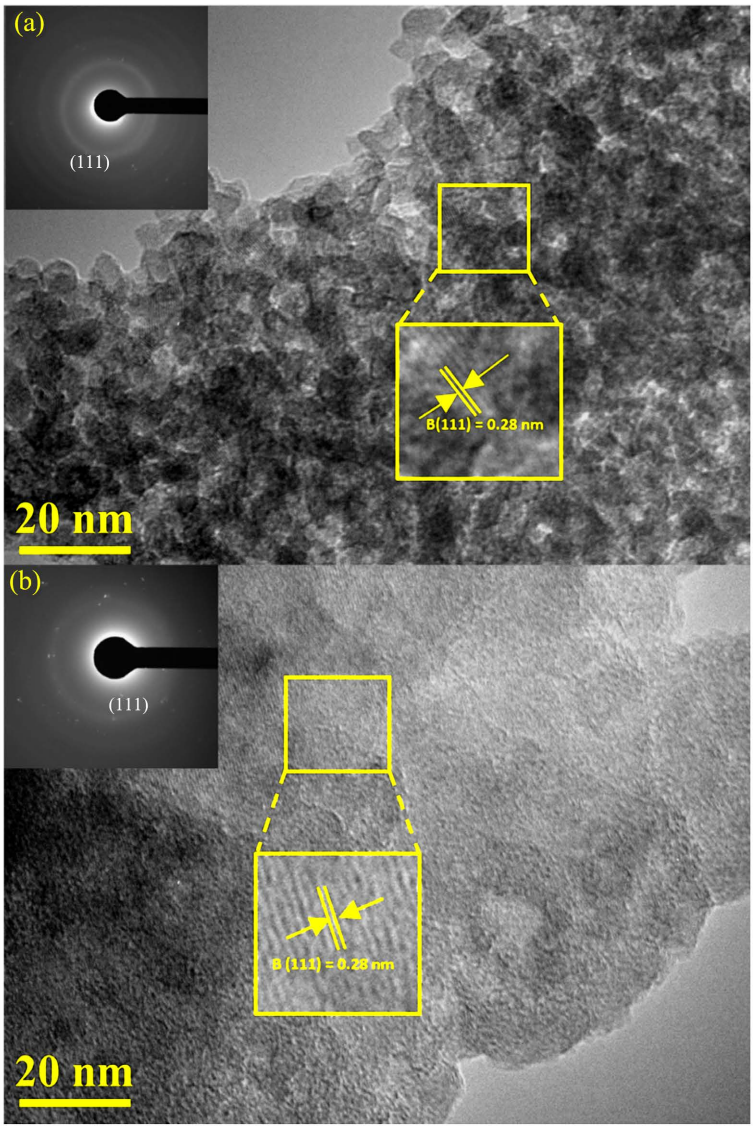

Figure 3. TEM images of the TiO_2 films treated at (a) 200˚C and (b) 300˚C; insets show corresponding SAED patterns.

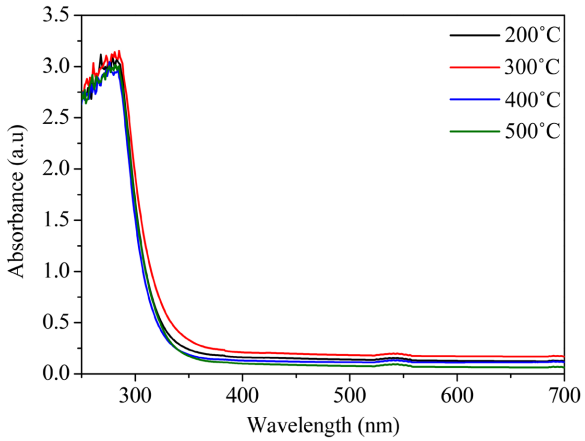

Figure 4. UV-Vis absorption spectra of the brookite TiO_2 coatings after heat treatment.

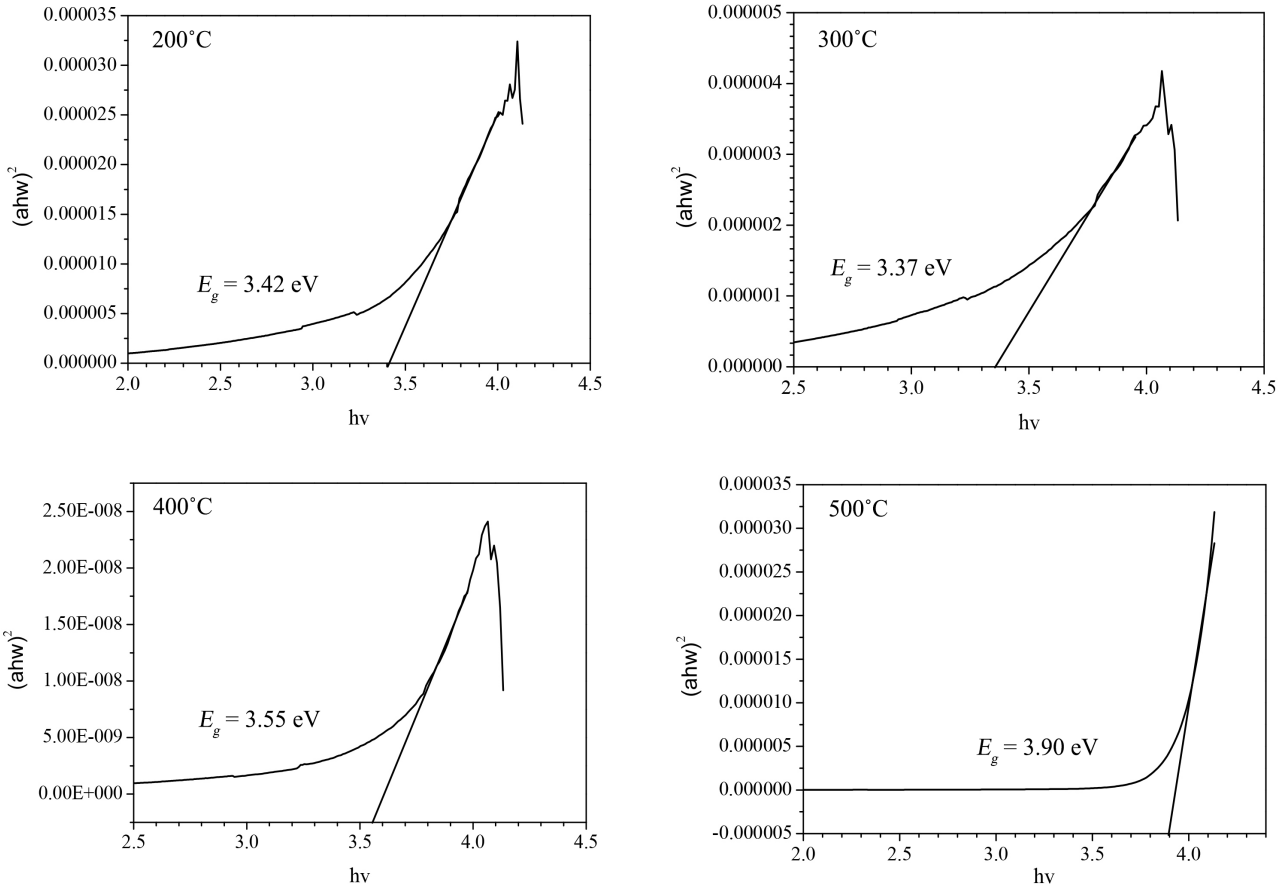

Figure 5. Optical band-gap estimates for the brookite TiO_2 coatings at different heat-treatment temperatures.

3.4. Photocatalytic Degradation of Methylene Blue under UV Irradiation

Under UV-C irradiation, the blank solution exhibited 18.5% apparent MB removal after 1 h and 38.1% after 4 h (**Figure 6**). The presence of a TiO_2 coating increased removal relative to the blank for every heat-treatment condition. After 4 h, the efficiencies were 63.0% at 200˚C, 67.7% at 300˚C, 62.0% at 400˚C, and 57.1% at 500˚C. At the 1 h point, the corresponding values were 38.4%, 44.9%, 38.8%, and 31.7%. The maximum four-hour removal was therefore obtained from the 300˚C film.

The superior UV-C result for the 300˚C film coincided with its largest calculated crystallite size among the crystalline specimens, 58.4 nm ± 12.0 nm, and with the strongest observed MB adsorption. Literature reports have connected photocatalytic response with crystallite dimensions over a broad range, approximately 1.67 - 67 nm [25]-[27], and crystallite size can influence both adsorption and charge transport [28]. The present data consequently support a relationship between structural development and activity at 300˚C, but they do not demonstrate that crystallite size alone determines the degradation rate.

The 300˚C sample also possessed the narrowest measured band gap, 3.37 eV. For comparison, Komaraiah *et al.* [27] reported 92.03% MB degradation from a

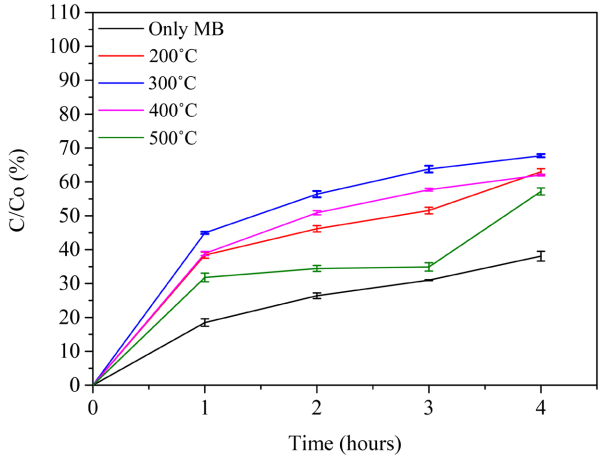

Figure 6. Methylene blue (MB) degradation under UV-C irradiation for TiO_2 films treated at different temperatures.

brookite TiO_2 thin film with a 3.30 eV band gap. The present 400˚C and 500˚C films gave lower four-hour removal values of 62.0% and 57.1%, respectively. Their structural states also differed: the 400˚C film retained a measurable 7.8 nm ± 1.0 nm crystallite size, whereas the 500˚C film was predominantly amorphous. The activity decrease at higher treatment temperatures therefore occurs together with changes in both crystallinity and the optical gap.

3.5. Photocatalytic Degradation of Methylene Blue under Visible-Light Irradiation

Under the reported visible-light condition, the blank solution reached 19.2% removal after 1 h and 28.9% after 4 h (**Figure 7**). All coated specimens performed better than the blank. Removal by the 300˚C film rose from 58.1% at 1 h to 97.8% at 4 h, while the 200˚C film increased from 34.3% to 95.4%. At 4 h, the 400˚C and 500˚C films reached 53.1% and 51.8%, respectively; their 1 h values were 35.0% and 32.6%. Thus, the four-hour order remained 300˚C > 200˚C > 400˚C > 500˚C.

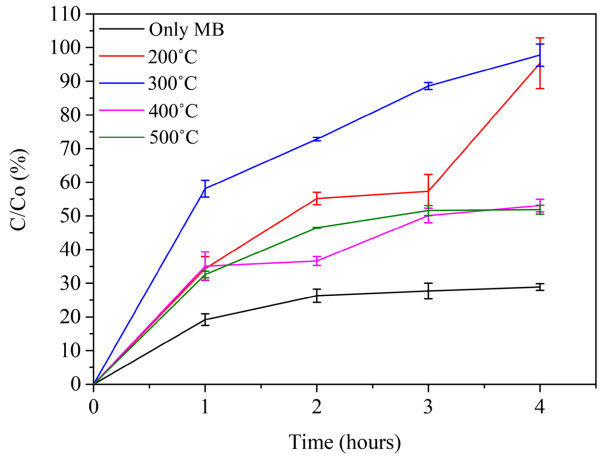

Figure 7. MB degradation under the reported visible-light condition for TiO_2 films treated at different temperatures.

For the 300˚C film, the measured crystallite size and optical gap were 58.4 nm ± 12.0 nm and 3.37 eV, respectively. The corresponding 200˚C values were 47.9 nm ± 19.9 nm and 3.42 eV, while the 400˚C specimen showed 7.8 nm ± 1.0 nm and 3.55 eV. The 500˚C coating, for which no crystalline domain size could be obtained from XRD, had the widest measured optical gap at 3.90 eV. The weaker visible-light response at 400˚C and 500˚C therefore coincided with both diminished crystalline development and a wider optical gap.

4. Discussion

4.1. Effect of Crystallite Size on Methylene Blue Degradation

A common trend emerges when the photocatalytic measurements are considered with the structural data: the 300˚C film was the most active under both irradiation conditions and also possessed the largest calculated crystallite size, 58.4 nm ± 12.0 nm. Its diffraction indicated the strongest crystalline development among the tested films. Since crystallinity and crystallite dimensions have previously been linked with TiO_2 photocatalysis [29]-[31], these observations provide a useful framework for discussing the temperature dependence measured in this work.

Earlier TiO_2 studies have demonstrated that photocatalytic behaviour can vary with crystal development. Tanaka *et al.* [29] reported a dependence of photocatalytic action on TiO_2 crystallinity, while Ohtani *et al.* [30] examined photocatalysis in amorphous-anatase systems. Armaković *et al.* [31] also found temperature-dependent photocatalytic performance in TiO_2-based materials. These reports support considering crystallinity as one contributor to the present activity trend, although the simultaneous changes in optical and surface properties mean that the individual contribution of crystallite size cannot be isolated from the current dataset.

4.2. Effect of Band-Gap Energy on Methylene Blue Degradation

The band-gap results provide another correlation with photocatalytic performance. The 300˚C film showed the smallest measured gap among the crystalline samples, 3.37 eV, and simultaneously delivered 67.7% UV-C and 97.8% visible-light MB removal after 4 h. In principle, a smaller optical gap can lower the photon-energy threshold associated with electronic excitation under suitable illumination. Nevertheless, this study did not independently determine carrier generation, recombination kinetics, or wavelength-specific absorption. The observed association should therefore be treated as evidence of correlation rather than proof that the band gap controls the degradation rate.

The conventional interpretation of TiO_2 photocatalysis involves photoexcitation followed by formation of electron-hole pairs. As described by Wang *et al.* [32], photogenerated electrons can participate in oxygen-reduction reactions that produce superoxide species, whereas photogenerated holes can drive oxidation processes involving water or surface hydroxyl groups. These species can subsequently contribute to organic-dye degradation. For the present films, however, no

direct measurements of radical concentration, carrier lifetime, or interfacial charge-transfer kinetics were performed. The pathway shown in Figure 8 should therefore be regarded as a literature-supported mechanistic interpretation of the MB-removal results, not as direct experimental proof of each elementary step.

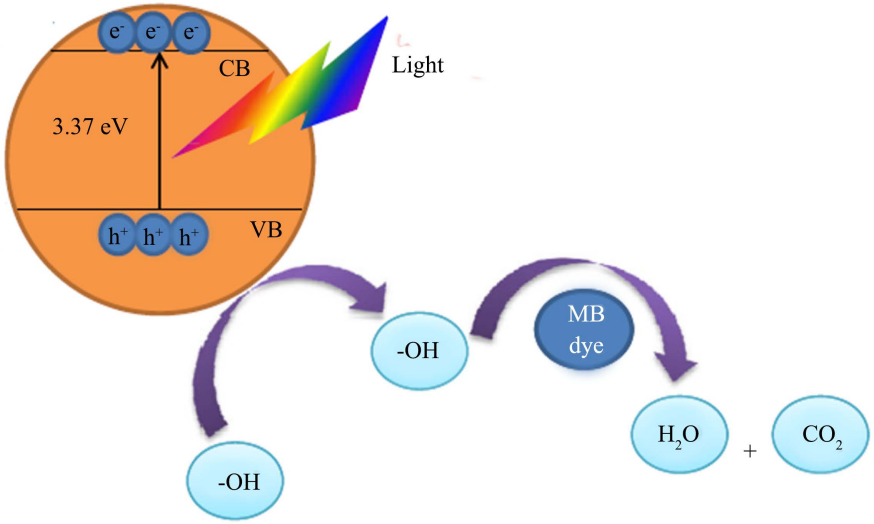

Figure 8. Schematic interpretation of the proposed photocatalytic pathway for the brookite TiO_2 film.

5. Conclusion

The thermal schedule altered all three classes of properties examined in this study: crystal structure, optical response, and photocatalytic behaviour. GAXRD showed detectable brookite as the only crystalline TiO_2 phase at 200˚C - 400˚C, whereas the 500˚C coating exhibited a predominantly amorphous pattern. TEM/SAED observations at 200˚C and 300˚C were consistent with brookite and showed an approximately 0.28 nm lattice spacing assigned to the (111) plane. The Scherrer-derived crystallite size increased from 47.9 nm ± 19.9 nm at 200˚C to 58.4 nm ± 12.0 nm at 300˚C, then decreased to 7.8 nm ± 1.0 nm at 400˚C. Optical-gap estimates were 3.42, 3.37, 3.55, and 3.90 eV at 200˚C, 300˚C, 400˚C, and 500˚C, respectively. The 300˚C film produced the highest four-hour MB removal under both test conditions, namely 67.7% under UV-C and 97.8% under the reported visible-light condition. The results therefore associate the optimum response with the combined structural and optical state obtained at 300˚C rather than with a single isolated parameter. Additional experiments that independently control crystallite size, optical absorption, and charge-transfer behaviour would be needed to establish their individual contributions.

Author Contributions

Jariah Mohamad Juoi: Conceptualization and Writing—Original Draft Preparation; **Nur Dalilah Johari:** Investigation, Data Curation, Formal Analysis, Methodology, Validation, and Writing—Review & Editing; **Zulkifli Mohd Rosli:** Su-

pervision, Validation, and Writing—Review & Editing. All authors contributed to the interpretation of the results, critically reviewed the manuscript, approved the final version of the manuscript, and agreed to be accountable for all aspects of the work.

Acknowledgements

The authors gratefully acknowledge the Faculty of Industrial and Manufacturing Technology and Engineering, Universiti Teknikal Malaysia Melaka (UTeM), for supporting this research.

Conflicts of Interest

The authors declare no conflicts of interest regarding the publication of this paper.

References

[1] Paul, S., Chetri, P., Choudhury, B., Ameen Ahmed, G. and Choudhury, A. (2015) Enhanced Visible Light Photocatalytic Activity of Gadolinium Doped Nanocrystalline Titania: An Experimental and Theoretical Study. *Journal of Colloid and Interface Science*, **439**, 54-61. https://doi.org/10.1016/j.jcis.2014.09.083

[2] Castro-Beltrán, A., Luque, P.A., Garrafa-Gálvez, H.E., Vargas-Ortiz, R.A., Hurtado-Macías, A., Olivas, A., *et al.* (2018) Titanium Butoxide Molar Ratio Effect in the TiO_2 Nanoparticles Size and Methylene Blue Degradation. *Optik*, **157**, 890-894. https://doi.org/10.1016/j.ijleo.2017.11.185

[3] Fujishima, A. and Honda, K. (1972) Electrochemical Photolysis of Water at a Semiconductor Electrode. *Nature*, **238**, 37-38. https://doi.org/10.1038/238037a0

[4] Di Paola, A., Bellardita, M. and Palmisano, L. (2013) Brookite, the Least Known TiO_2 Photocatalyst. *Catalysts*, **3**, 36-73. https://doi.org/10.3390/catal3010036

[5] Monai, M., Montini, T. and Fornasiero, P. (2017) Brookite: Nothing New under the Sun? *Catalysts*, **7**, Article 304. https://doi.org/10.3390/catal7100304

[6] Rahimi, N., Pax, R.A. and Gray, E.M. (2016) Review of Functional Titanium Oxides. I: TiO_2 and Its Modifications. *Progress in Solid State Chemistry*, **44**, 86-105. https://doi.org/10.1016/j.progsolidstchem.2016.07.002

[7] Kaplan, R., Erjavec, B., Dražić, G., Grdadolnik, J. and Pintar, A. (2016) Simple Synthesis of Anatase/Rutile/Brookite TiO_2 Nanocomposite with Superior Mineralization Potential for Photocatalytic Degradation of Water Pollutants. *Applied Catalysis B: Environmental*, **181**, 465-474. https://doi.org/10.1016/j.apcatb.2015.08.027

[8] Han, X., Han, X., Sun, L., Wang, P., Jin, M. and Wang, X.J. (2016) Facile Preparation of Hybrid Anatase/Rutile TiO_2 Nanorods with Exposed (010) Facets for Lithium Ion Batteries. *Materials Chemistry and Physics*, **171**, 11-15. https://doi.org/10.1016/j.matchemphys.2015.11.048

[9] Johari, N.D., Rosli, Z.M., Juoi, J.M. and Yazid, S.A. (2019) Comparison on the TiO_2 Crystalline Phases Deposited via Dip and Spin Coating Using Green Sol-Gel Route. *Journal of Materials Research and Technology*, **8**, 2350-2358. https://doi.org/10.1016/j.jmrt.2019.04.018

[10] Djaoued, Y., Brüning, R., Bersani, D., Lottici, P.P. and Badilescu, S. (2004) Sol-Gel Nanocrystalline Brookite-Rich Titania Films. *Materials Letters*, **58**, 2618-2622. https://doi.org/10.1016/j.matlet.2004.03.034

[11] Bergamonti, L., Alfieri, I., Lorenzi, A., Montenero, A., Predieri, G., Di Maggio, R., *et al.* (2015) Characterization and Photocatalytic Activity of TiO_2 by Sol-Gel in Acid and Basic Environments. *Journal of Sol-Gel Science and Technology*, **73**, 91-102. https://doi.org/10.1007/s10971-014-3498-y

[12] Kandiel, T.A., Robben, L., Alkaima, A. and Bahnemann, D. (2013) Brookite versus Anatase TiO_2 Photocatalysts: Phase Transformations and Photocatalytic Activities. *Photochemical & Photobiological Sciences*, **12**, 602-609. https://doi.org/10.1039/c2pp25217a

[13] Tran, H.T.T., Kosslick, H., Ibad, M.F., Fischer, C., Bentrup, U., Vuong, T.H., *et al.* (2017) Photocatalytic Performance of Highly Active Brookite in the Degradation of Hazardous Organic Compounds Compared to Anatase and Rutile. *Applied Catalysis B*: *Environmental*, **200**, 647-658. https://doi.org/10.1016/j.apcatb.2016.07.017

[14] Alotaibi, A.M., Sathasivam, S., Williamson, B.A.D., Kafizas, A., Sotelo-Vazquez, C., Taylor, A., *et al.* (2018) Chemical Vapor Deposition of Photocatalytically Active Pure Brookite TiO_2 Thin Films. *Chemistry of Materials*, **30**, 1353-1361. https://doi.org/10.1021/acs.chemmater.7b04944

[15] Manjumol, K.A., Jayasankar, M., Vidya, K., Mohamed, A.P., Nair, B.N. and Warrier, K.G.K. (2015) A Novel Synthesis Route for Brookite Rich Titanium Dioxide Photocatalyst Involving Organic Intermediate. *Journal of Sol-Gel Science and Technology*, **73**, 161-170. https://doi.org/10.1007/s10971-014-3507-1

[16] Haggerty, J.E.S., Schelhas, L.T., Kitchaev, D.A., Mangum, J.S., Garten, L.M., Sun, W., *et al.* (2017) High-Fraction Brookite Films from Amorphous Precursors. *Scientific Reports*, **7**, Article No. 15232. https://doi.org/10.1038/s41598-017-15364-y

[17] Allen, N.S., Mahdjoub, N., Vishnyakov, V., Kelly, P.J. and Kriek, R.J. (2018) The Effect of Crystalline Phase (Anatase, Brookite and Rutile) and Size on the Photocatalytic Activity of Calcined Polymorphic Titanium Dioxide (TiO_2). *Polymer Degradation and Stability*, **150**, 31-36. https://doi.org/10.1016/j.polymdegradstab.2018.02.008

[18] Li, Y., White, T.J. and Lim, S.H. (2004) Low-Temperature Synthesis and Microstructural Control of Titania Nano-Particles. *Journal of Solid State Chemistry*, **177**, 1372-1381. https://doi.org/10.1016/j.jssc.2003.11.016

[19] Liao, M.Y., Fang, L., Xu, C.L., Wu, F., Huang, Q.L. and Saleem, M. (2014) Effect of Seed Layer on the Growth of Rutile TiO_2 Nanorod Arrays and Their Performance in Dye-Sensitized Solar Cells. *Materials Science in Semiconductor Processing*, **24**, 1-8. https://doi.org/10.1016/j.mssp.2014.02.037

[20] Herman, G.S., Dohnálek, Z., Ruzycki, N. and Diebold, U. (2003) Experimental Investigation of the Interaction of Water and Methanol with Anatase-TiO_2 (101). *The Journal of Physical Chemistry B*, **107**, 2788-2795. https://doi.org/10.1021/jp0275544

[21] Taylor, K.M.G. and Aulton, M.E. (2017) Aulton's Pharmaceutics E-Book: The Design and Manufacture of Medicines. 5th Edition, Elsevier Health Sciences.

[22] Khan, M.I., Bhatti, K.A., Qindeel, R., Althobaiti, H.S. and Alonizan, N. (2017) Structural, Electrical and Optical Properties of Multilayer TiO_2 Thin Films Deposited by Sol-Gel Spin Coating. *Results in Physics*, **7**, 1437-1439. https://doi.org/10.1016/j.rinp.2017.03.023

[23] Verma, R., Mantri, B. and Srivastava, K.A. (2015) Shape Control Synthesis, Characterizations, Mechanisms and Optical Properties of Larg Scaled Metal Oxide Nanostructures of ZnO and TiO_2. *Advanced Materials Letters*, **6**, 324-333. https://doi.org/10.5185/amlett.2015.5661

[24] Shi, Y., Zhang, R., Zheng, H., Li, D., Wei, W., Chen, X., *et al.* (2017) Optical Constants and Band Gap Evolution with Phase Transition in Sub-20-nm-Thick TiO_2 Films Pre-

pared by ALD. *Nanoscale Research Letters*, **12**, Article No. 243. https://doi.org/10.1186/s11671-017-2011-2

[25] Nandiyanto, A.B.D., Zaen, R. and Oktiani, R. (2020) Correlation between Crystallite Size and Photocatalytic Performance of Micrometer-Sized Monoclinic WO_3 Particles. *Arabian Journal of Chemistry*, **13**, 1283-1296. https://doi.org/10.1016/j.arabjc.2017.10.010

[26] Krýsa, J., Novotná, P., Kment, Š. and Mills, A. (2011) Effect of Glass Substrate and Deposition Technique on the Properties of Sol Gel TiO_2 Thin Films. *Journal of Photochemistry and Photobiology A*: *Chemistry*, **222**, 81-86. https://doi.org/10.1016/j.jphotochem.2011.05.005

[27] Komaraiah, D., Madhukar, P., Vijayakumar, Y., Reddy, M.R. and Sayanna, R. (2016) Photocatalytic Degradation Study of Methylene Blue by Brookite TiO_2 Thin Film under Visible Light Irradiation. *Materials Today*: *Proceedings*, **3**, 3770-3778. https://doi.org/10.1016/j.matpr.2016.11.026

[28] Yuangpho, N., Trinh, D.T.T., Channei, D., Khanitchaidecha, W. and Nakaruk, A. (2018) The Influence of Experimental Conditions on Photocatalytic Degradation of Methylene Blue Using Titanium Dioxide Particle. *Journal of the Australian Ceramic Society*, **54**, 557-564. https://doi.org/10.1007/s41779-018-0184-5

[29] Tanaka, K., Capule, M.F.V. and Hisanaga, T. (1991) Effect of Crystallinity of TiO_2 on Its Photocatalytic Action. *Chemical Physics Letters*, **187**, 73-76. https://doi.org/10.1016/0009-2614(91)90486-s

[30] Ohtani, B., Ogawa, Y. and Nishimoto, S.I. (1997) Photocatalytic Activity of Amorphous-Anatase Mixture of Titanium(IV) Oxide Particles Suspended in Aqueous Solutions. *The Journal of Physical Chemistry B*, **101**, 3746-3752. https://doi.org/10.1021/jp962702+

[31] Armaković, S.J., Grujić-Brojčin, M., Šćepanović, M., Armaković, S., Golubović, A., Babić, B., *et al.* (2019) Efficiency of La-Doped TiO_2 Calcined at Different Temperatures in Photocatalytic Degradation of β-Blockers. *Arabian Journal of Chemistry*, **12**, 5355-5369. https://doi.org/10.1016/j.arabjc.2017.01.001

[32] Wang, W., Serp, P., Kalck, P. and Faria, J.L. (2005) Visible Light Photodegradation of Phenol on MWNT-TiO_2 Composite Catalysts Prepared by a Modified Sol-Gel Method. *Journal of Molecular Catalysis A*: *Chemical*, **235**, 194-199. https://doi.org/10.1016/j.molcata.2005.02.027